Human Reproduction Vol.21, No.5 pp. 1194–1203, 2006 doi:10.1093/humrep/dei479
Advance Access publication February 22, 2006.

An azoospermic man with a double-strand DNA break-processing deficiency in the spermatocyte nuclei: Case report

R.B.Sciurano[1], M.I.Rahn[1], M.I.Pigozzi[1], S.Brugo Olmedo[2] and Alberto J.Solari[1,3]

[1]Facultad de Medicina, Centro de Investigaciones en Reproducción (CIR) and [2]CEGYR, Viamonte, Buenos Aires, Argentina

[3]To whom correspondence should be addressed at: Facultad de Medicina, CIR, Paraguay 2155, 11219 Buenos Aires, Argentina. E-mail: ajsolari@mail.retina.ar

BACKGROUND: The mechanisms of meiotic arrest in human spermatogenesis are poorly known. METHODS AND RESULTS: A testicular biopsy from an azoospermic male showed complete spermatogenesis arrest at the spermatocyte stage, asynapsis, lack of formation of the XY body, partial reversion to a mitotic-like division and cell degeneration both at the prophase and at the abnormal cell divisions. Synaptonemal complex analysis showed minor segments of synapsis and mainly single axes. Fluorescent immunolocalization of meiotic proteins showed normal SYCP3, scarcity of SYCP1, null MLH1 foci, about 10 patches of γ-H2AX, abnormal presence of BRCA1 among autosomal axes, absence of RAD51 in early and advanced spermatocytes and permanence of γ-H2AX labelling up to the abnormal spermatocyte divisions that are the most advanced stage reached. There are at least six dominions of evenly packed chromatin resembling that of the normal XY body, but no true XY body. CONCLUSIONS: The protein phenotype and the fine structure of the nuclei are compatible with a deficiency of the processing of double-strand DNA breaks in the zygotene-like spermatocytes, but the features of this defect do not agree with Spo11, Sycp1, Atm and Dmc1 null mutations, which give absence of XY body, synapsis disturbances and spermatocyte apoptosis in mice.

Key words: asynapsis/azoospermia/double-strand DNA breaks/meiotic arrest/SPO11

Introduction

Spermatogenic arrest at meiotic prophase is a common finding in testicular biopsies of azoospermic patients (Schulze *et al*., 1999). Among these azoospermic patients, in those having germ cell populations (i.e. discarding Sertoli cell-only syndrome), a significant fraction corresponds to genetic disturbances, both chromosomal (reviewed in Speed, 1989; Van Assche *et al*., 1996) and genic (Escalier, 2001). Chromosomal rearrangements and aneuploidy are well known as sources of spermatogenic arrest at meiotic prophase as ascertained with synaptonemal complex analysis (Speed, 1989; Solari, 1999). On the other hand, gene disturbances are less understood, and it is only in recent years that definite gene defects have been proved or suggested as the origin of meiotic arrest in human spermatogenesis (Miyamoto *et al*., 2003; Judis *et al*., 2004; Sun *et al*., 2004). Recent data on mouse spermatogenesis have significantly improved the general knowledge of gene actions in spermatocyte meiosis (Barchi *et al*., 2005; Bellani *et al*., 2005; Kolas *et al*., 2005; Turner *et al*., 2005). Null mutations of the main proteins of the synaptonemal complex, SYCP1 and SYCP3, originate spermatogenesis arrest in mice (de Vries *et al*., 1999; Yuan *et al*., 2000) and in man (Miyamoto *et al*., 2003).

Furthermore, the basic meiotic genes: Spo11 (Baudat *et al*., 2000; Romanienko and Camerini-Otero, 2000), Dmc1 (Pittman *et al*., 1998; Yoshida *et al*., 1998), γ-H2ax (Celeste *et al*., 2002), Msh5 (Edelmann *et al*., 1999) and Mlh1 (Edelmann *et al*., 1996) and the kinase ATM (Xu *et al*., 1996) are also needed for the normal development of meiotic prophase in mouse spermatocytes. The basic recombinase RAD51 is also relevant in mammalian meiotic prophase, as it co-localizes with DMC1 during meiotic prophase (reviewed by Masson and West, 2001), but its meiotic role is more difficult to assess, as its null mutation is lethal (Tsuzuki *et al*., 1996). The interplay of these meiotic proteins with other factors in mouse meiosis is rapidly advancing (Turner *et al*., 2004; Barchi *et al*., 2005) and opens new viewpoints for human meiotic arrest in azoospermic patients.

This case is that of an azoospermic man who shows complete spermatogenesis arrest at the spermatocyte level with cell degeneration and death at meiotic prophase and cell division. The analysis of microspread spermatocytes under electron microscopy (EM) shows a high degree of asynapsis, with full formation of chromosomal axes that mainly do not form synaptonemal complexes except at very minor, terminal regions. Thin sections confirm the very scarce formation of tiny paired regions at the nuclear periphery and the absence of the characteristic

XY body of normal pachytene spermatocytes (Solari, 1974, 1980, 1999). The protein phenotype of these spermatocytes, ascertained with immunolocalization, shows the presence of abundant patches of γ-H2AX indicating the presence of double-strand breaks (DSBs) of DNA along most of the single axes, which are positive for the regulating protein BRCA1 all along their path, and normal presence of the main axial protein SYCP3, but only short traces of the main protein of the transverse filaments, SYCP1. The recombinase RAD51 and the late-acting repair protein MLH1 are completely lacking in the spermatocytes of the patient. Some of the spermatocytes enter an abortive cell division that shows univalents and γ-H2AX labelling. The protein phenotype and the added morphological details are compatible with a deficiency in the processing of DNA breaks originated by SPO11, as already described in the mouse (Barchi *et al*., 2005) but having no counterpart in the already described null mutants of mice.

Case report

The patient is an apparently healthy man of 33 years of age referred to an infertility clinic. The physical examination and the instrumental data excluded an obstructive source of the azoospermia. FSH plasmatic level was 7.6 IU, and other analyses were within normal ranges. The karyotype from peripheral blood lymphocytes showed 46, XY with a heterozygous pericentric inversion in chromosome 2, inv 2 (p11;q13). This same inversion was found in the mother of the propositus.

A bilateral testicular biopsy was performed for histopathological diagnosis and for the possibility of performing ICSI. The tissue was divided in pieces for light and EM and for protein immunolocalization. All the research procedures in this case were submitted and accepted through the ethics committee of the School of Medicine [Facultad de Medicina, Comite Independiente de Etica de Investigación (CIEI), UBA, Buenos Aires, Argentina]. Testicular biopsies from three men having complete spermatogenesis were used as controls for the immunolocalization of meiotic proteins. As regards the fine structure of spermatocytes used as controls, this laboratory has studied approximately 45 biopsies of men (Solari, 1980, 1999).

For light microscopy, a piece of tissue was fixed in Bouin's fixative, embedded in paraffin and stained with haematoxylin and eosin (H–E) as the routine procedure. For EM, microspreads for synaptonemal complex analysis were performed, as previously described (Solari, 1998), and stained with silver nitrate (Howell and Black, 1980). For 3D reconstruction with EM, serial sections from epoxy-embedded tissue were collected in single-hole grids (Solari, 1998), stained with uranyl acetate and lead citrate, and micrographs obtained using a Siemens electron microscope (Siemens AG, Berlin, Germany). The scanned profiles of nuclear structures were processed with the IGL TRACE program (John C. Fiala, copyright 2001) for 3D reconstruction and saved with a GL VIEW 3.0 viewer (Holger Grahn, copyright 2001), as previously described (Solari *et al*., 2003).

Immunolocalization

Spermatocyte microspreads were fixed with 1% formaldehyde, and the slides were kept at –70°C until used for fluorescence microscopy. Slides were blocked with PBT [0.15% bovine serum albumin (BSA) and 0.1% Tween-20 in phosphate-buffered saline (PBS)] for 30 min at room temperature before incubation with primary antibodies. The following primary antibodies, diluted in PBT, were incubated overnight (ON) at 37°C: a mouse anti-γ-H2AX (Upstate Biotech, Lake Placid, NY, USA) at 1:1000 dilution, a rabbit anti-BRCA1 (Santa Cruz Biotech, CA, USA) at 1:50, a rabbit anti-RAD51 (Santa Cruz Biotech) at 1:20 and a rabbit anti-MLH1 (Oncogene, Science, San Diego, CA, USA) at 1:30. The rabbit anti-SYCP1 antibody (P.J. Moens, York U, Toronto, Ontario, Canada) diluted in PBT at 1:400 dilution and a mouse anti-SYCP3 antibody (D. Camerini-Otero, NIDDK, NIH) at 1:200 were incubated ON at 4°C. All incubations were performed in a humid chamber. After washing, secondary antibodies, fluorescein isothiocyanate (FITC)-labelled goat anti-rabbit and tetramethylrhodamine isothiocyanate (TRITC)-labelled goat anti-mouse, were used at 1:50 dilution in PBT. Slides were counterstained with 4(,6-diamidino-2-phenylindole) (DAPI) and mounted in glycerol with 1,4-diazobicyclo-(2,2,2)-octane (DABCO) antifade.

For immunolocalization, spreads were examined with a LEICA DM microscope (Leica Microsystems, Wetzlar, Germany) with the corresponding filters and photographed with Agfa color 400 ASA 35 mm film (AGFA-Gevaert, Leverkusen, Germany). Two exposures were done sequentially on the same frame: one using the FITC filter and the other with Rhodamine filter. Previous tests gave no differences between this method and the superimposition of separate images.

Results

Light microscopy of semi-thin sections

Semi-thin (1-μm thick) sections showed full spermatogenic arrest at the spermatocyte stage. No spermatids or sperm were observed in any seminiferous tubule in semi-thin or in routine paraffin sections. The most advanced stages in these tubules are abnormal cell divisions of the spermatocytes near the lumen of the tubuli (Figure 1). Cell degeneration and death, as indicated by nuclear pycnosis, nuclear fragmentation and homogeneous or highly vacuolated cytoplasm, were observed at two distinct stages, the first one at meiotic prophase in the more advanced pseudo-zygotene spermatocytes and the second one at the abnormal spermatocyte divisions. While the spermatogonia, Sertoli cells and the earlier (leptotene) spermatocyte stages had a normal appearance, no true pachytene or diplotene spermatocytes could be shown in the biopsy (Figure 1). Instead, a large number of zygotene-like spermatocytes form the majority of germ cells in the tubuli. These pseudo-zygotene spermatocytes have less dense chromatin threads compared with normal pachytene cells, but they have similar nuclear sizes. In fact, as shown by EM (see: *EM sections*), these cells have almost fully unpaired chromosomal axes. A typical XY body is also lacking in these nuclei.

The abnormal spermatocyte divisions are located near or at the lumen and form a significant number of the germinal cells. They appear located as groups of dividing cells in some of the tubuli. However, the chromosomes lack any ordered pattern, being scattered in the cytoplasm, which also lacks any spindle structures. These abnormalities are confirmed by EM observations (see: *EM sections*).

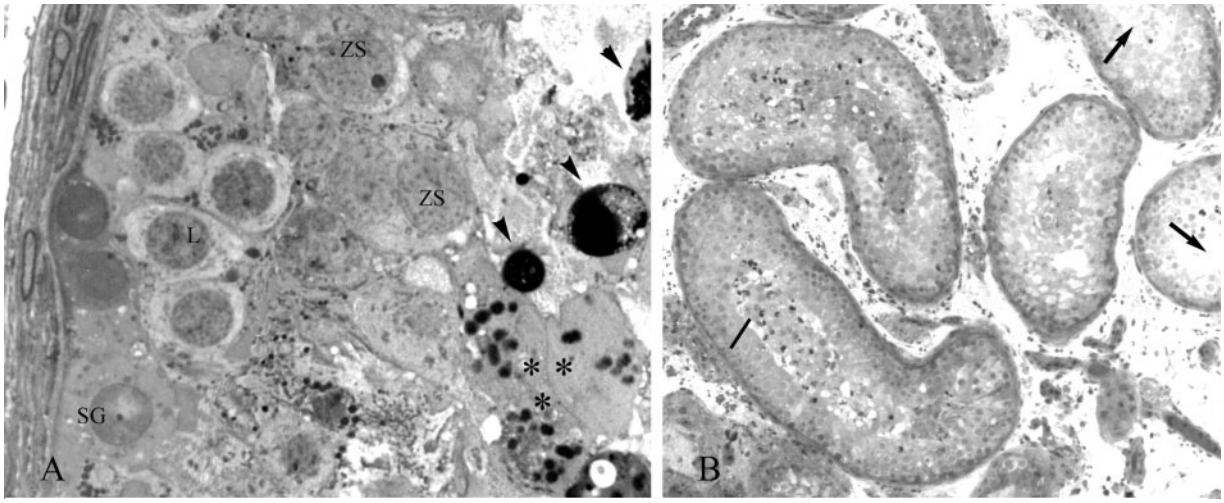

Figure 1. (**A**–**B**) Semi-thin (1-μm thick) section of the testicular biopsy. (**A**) Spermatogonia (SG) and leptotene spermatocytes (L) show normal morphology. There are many zygotene-like spermatocytes (ZS) and complete absence of pachytene spermatocytes. Abnormal cell divisions (asterisks) are near the lumen. Nuclear pycnosis (arrowheads) shows cell death. (**B**) Tubules without advanced spermatocytic stages (arrows) and tubules with abnormal cell divisions and apoptosis (line). Magnification: (**A**) ×960 and (**B**) ×180.

Synaptonemal complex (SC) analysis

Spermatocyte spreads showed a very typical pattern: full formation of single chromosomal axes, generalized lack of full synapsis, lack of an XY body and scattered nucleolar material. Among 100 spermatocytes analysed in micrographs and several hundred observed directly in the EM, none had a full set of synaptonemal complexes. In fact, the typical spermatocyte has only single axes (Figure 2A) which may have the terminal plaques as expansions at both ends, although many of the axes lack clear terminal expansions. Many eye-like localized splits are observed in the single axes of most of these cells (Figure 3). As in some of these cells, there were short stretches of apparent SCs, an analysis was made on the extent of paired axes in the whole sample and the frequency of fully paired axes (Table I and Figure 4). As shown in Table I and Figure 4, the average spermatocyte has little or no SCs. Whenever SCs are present, they frequently show non-homologous associations (Figure 2B). Short stretches of SCs are preferentially located at axial termini. The most advanced development of SCs in the whole sample covers only a minor fraction of the chromosomal complement.

Another abnormality is the absence of the fully developed nucleoli proper of pachytene cells. Instead, nucleolar-like material is scattered throughout the nucleus, although with some preference for the location near some of the axial termini. No XY-paired axes were observed in the full sample, and no broken SCs or abnormal segments of thickened or disjoined axes were noticed.

EM sections

To validate the observations in spreads, epoxy-embedded thin sections were examined under EM. The sections confirmed that the most advanced stage of meiotic prophase of the spermatocytes is a zygotene-like stage in which the large nucleus shows many single, unpaired axes, which end on the inner surface of the nuclear envelope without any regular bouquet-like orientation (Figure 5A). A minor frequency of ends showed pieces of SCs which are apparently equal to those of normal SCs (Figure 5B). In fact, the presence of a central element and transverse filaments can be assessed in these short terminal pieces of SCs. These observations agree with the results of immunolocalization of the main protein of the transverse filaments, SYCP1 (see: *Immunolocalization of meiotic proteins*). Well-developed nucleoli with the segregated main regions as in normal pachytene cells (reviewed in Solari, 1993) were not observed in these sections. Instead, cumuli of nucleolar-like, granular material was dispersed in the spermatocyte nuclei. No XY body was observed in thin sections, and partial 3D reconstructions of these spermatocyte nuclei revealed no traces of the true XY body with the characteristic gonosomal axes (reviewed in Solari, 1993). Instead, patches of evenly packed chromatin, different from most of the nuclear chromatin, which numbered 8–10 in the partially reconstructed nuclei, were similar to the specific chromatin packing of the normal XY body. These chromatin patches did not associate with the nuclear envelope (as it does the normal XY body), but they have single axes associated to their central regions. None of these patches could be identified with a sex chromosome.

The abnormal spermatocyte divisions (Figure 5C) were definitely different from the normal meiotic divisions of human spermatocytes. They do not have a mitotic apparatus: there are no microtubuli attached to any of the chromosomes, nor any polar regions with converging microtubules. Furthermore, the chromosomes were disordered, without the regular appearance of meiotic metaphase plates. In fact, the chromosomes may be surrounded by vacuoles or aggregated in several cumuli, without any spatial relationship. The cytoplasm is full of abnormal hydrophilic-like vacuoles. Some vacuoles appear packed as a somewhat irregular lattice, which in 3D corresponds to packed polyhedra (Figure 5D). Some of these cell divisions showed signs of degeneration as chromatin clumping

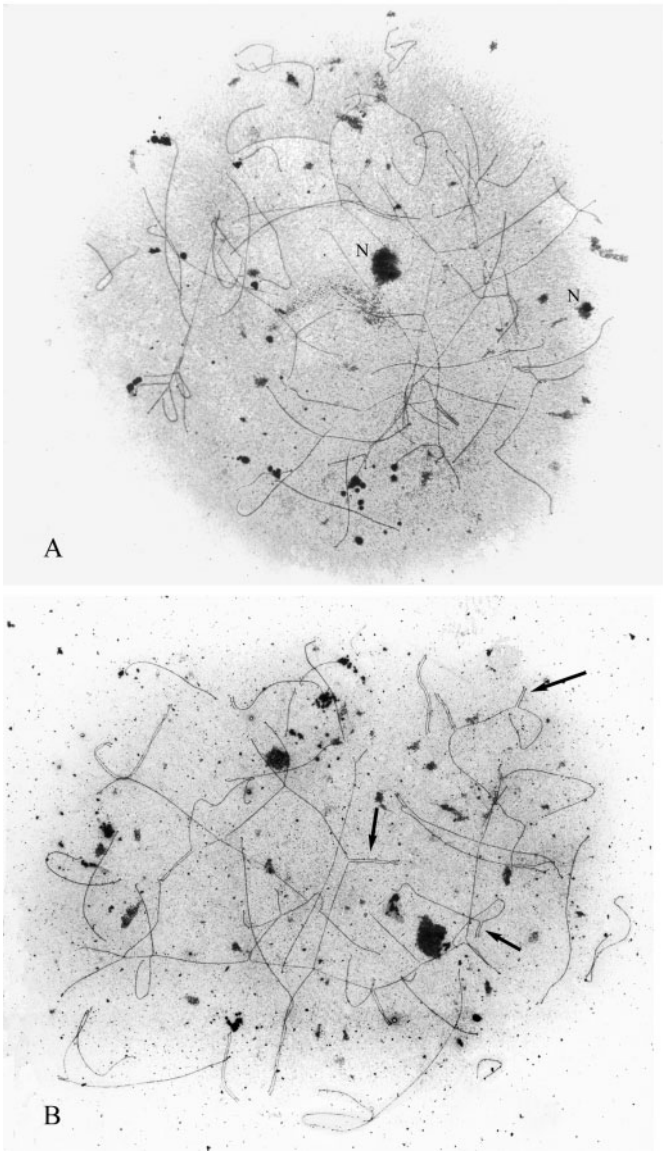

Figure 2. (**A**–**B**) Electron micrographs of spermatocyte spreads. (**A**) Typical zygotene-like spermatocyte, showing single axes and patches of nucleolar material (N). (**B**) Maximum synapsis observed among 100 spread spermatocytes. Some instances of non-homologous synapsis are marked by arrows. Silver staining. Magnification: (**A**) ×2950 and (**B**) ×2700.

in almost amorphous masses. No regular, daughter-cell-like products were observed.

Cytogenetic spreads

Spreads using the routine spreading technique for meiotic chromosomes showed a small quantity of normal spermatogonial mitoses (2n = 46) and a much higher frequency of abnormal divisions. These were quite different from meiotic divisions, as no chiasmata were seen in any cell, and no regular distribution of the chromosomes either in metaphase plates or in anaphase groups could be observed. In fact, the modal chromosome number in these abnormal cells was about 46 (mean = 46.4; SD = 2.5; n = 11), and the other group had a modal number of about 92. The chromosomes were ill delineated, with fuzzy outlines, as observed in degenerating cells. In some cases, similar-sized chromosomes lay side by side, as homologues, but no chiasmatic connections were seen between them.

Figure 3. Electron micrograph showing details of the single axes in the zygotene-like spermatocytes. The arrowhead marks the unusual 'eye-like' splits. The ends of the axis show the typical terminal expansions (asterisks). Silver staining. Magnification: ×4500.

Table I. Average total lengths of single axes and synapsed segments in a sample of 30 zygotene-like spermatocytes

	Mean (range)
Absolute total lengths of single axes (μm)	480.14 (283.87–577.62)
Absolute total lengths of synapsed segments (μm)	26.55 (0–181.48)
Lengths of synapsed segments (%)	6.11 (0–43.97)
Total number of synapsed segments	7 (0–28)
Number of complete synapsed bivalents	1.6 (0–12)

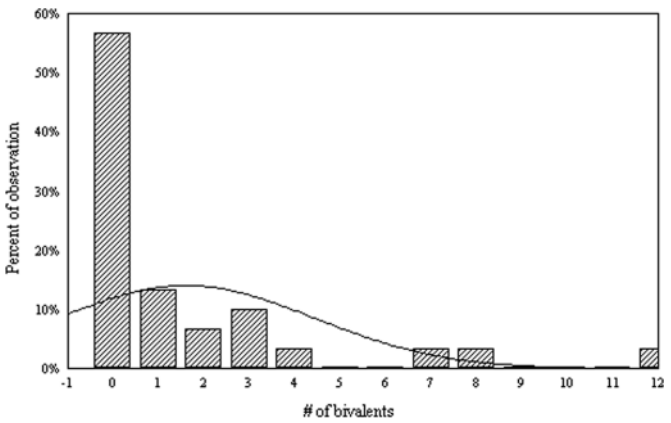

Figure 4. Histogram showing the frequency of the total number of synapsed homologues in the zygotene-like cells.

Immunolocalization of meiotic proteins

Immunolocalization of the SC components: SYCP3 and SYCP1

SYCP3, the main protein component of the lateral elements of SCs, is present all along the single axes of the spermatocytes (Figure 6A). The examination of several hundred spermatocytes with fluorescent immunolocalization of SYCP3 confirmed the

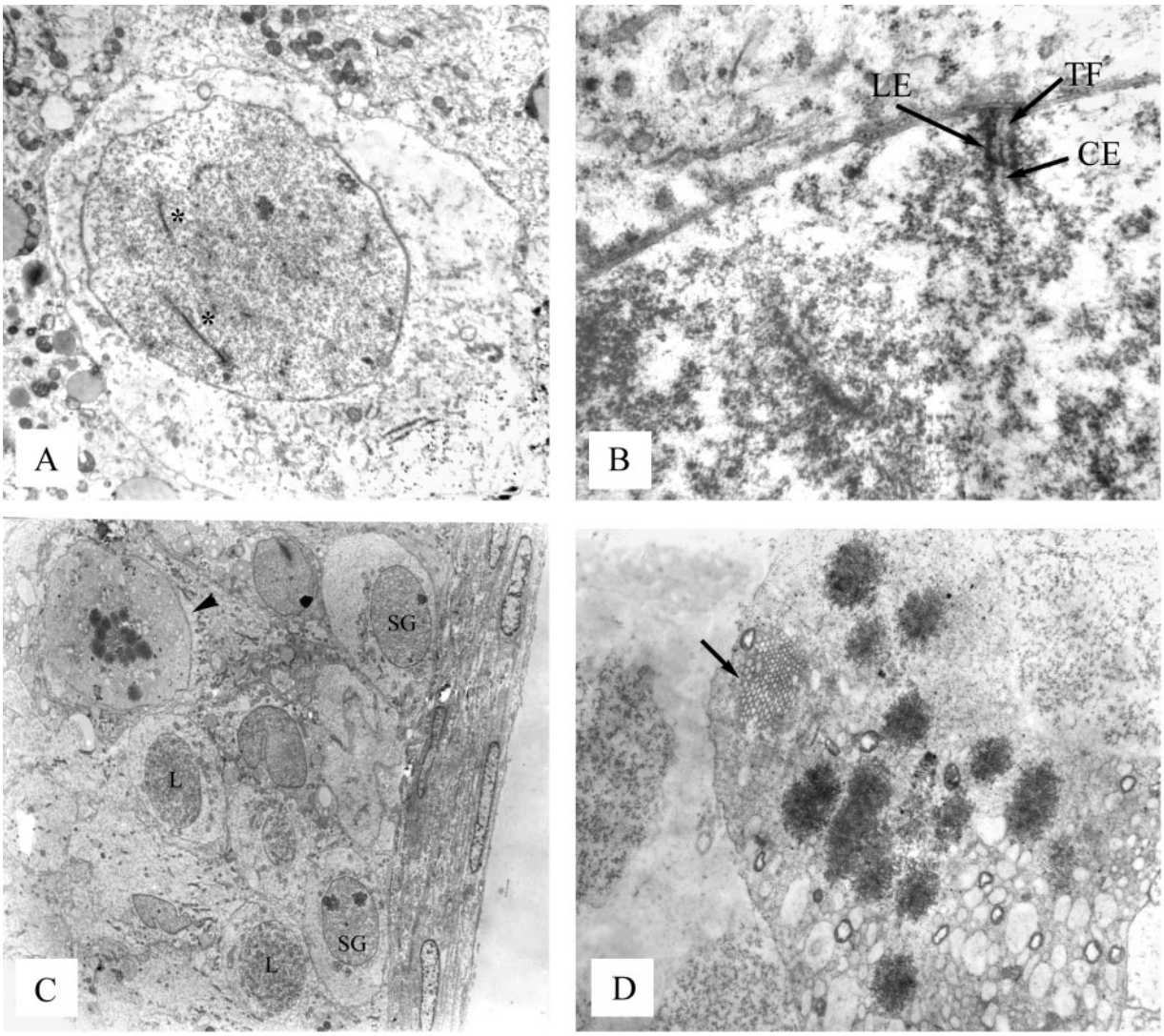

Figure 5. (**A**–**D**) Electron micrographs of thin sections from the testicular biopsy. (**A**) Typical zygotene-like cell showing single axes (asterisks). Magnification: ×5000. (**B**) A terminal segment of an infrequent synaptonemal complex, showing the lateral elements (LE), the central element (CE) and the normal transverse filaments (TF). Magnification: ×21 000. (**C**) Low-magnification electron micrograph showing normal spermatogonia (SG) and leptotenes (L) and one abnormal cell division (arrowhead) near the lumen. Magnification: ×1900. (**D**) Electron micrograph of one abnormal spermatocyte division showing the absence of microtubuli, the abundant clear vacuoles and the lattice-like array of small vacuoles. Magnification: ×4700.

fact that no true pachytene cells are present in this patient, as none had the normal complement of 22 bivalents and the sex pair. Instead, most of the spermatocytes had single axes without any specific arrangement. The simultaneous immunolocalization of the main component of the transverse filaments (SYCP1) showed short stretches of paired axes, mainly at the nuclear periphery (Figure 6B), confirming the actual presence of this SC component as well as the paucity of synapsis among the chromosomal axes.

Immunolocalization of γ-H2AX and BRCA1

The variant histone γ-H2AX, which is usually considered as a marker of DSBs, was present as numerous small patches during leptotene. In the majority of the spermatocytes, blocked at the pseudo-zygotene stage, γ-H2AX was present as a series of patches (Figure 6C) scattered over the nucleus, but without the formation of the large XY, γ-H2AX domain of normal pachytenes (Figure 6D). Simultaneous immunolocalization of BRCA1 showed the abnormal presence of this protein decorating the single axes (Figure 6C). Thus, single axes decorated with BRCA1 lay at the centre of γ-H2AX patches, and some chromatin regions devoid of γ-H2AX. No X or Y axes decorated with BRCA1 were observed, in contrast to normal (control) spermatocytes (Figure 6D).

Chromatin patches with γ-H2AX were present also in the abnormal spermatocyte divisions (Figure 6E). In fact, the variant histone γ-H2AX was co-localized with most, but not all, scattered chromosomes of the abnormal cell divisions (Figure 6E).

Immunolocalization of RAD51 protein

Contrary to controls in which RAD51 was present as series of foci along the axes of leptotene and zygotene chromosomes

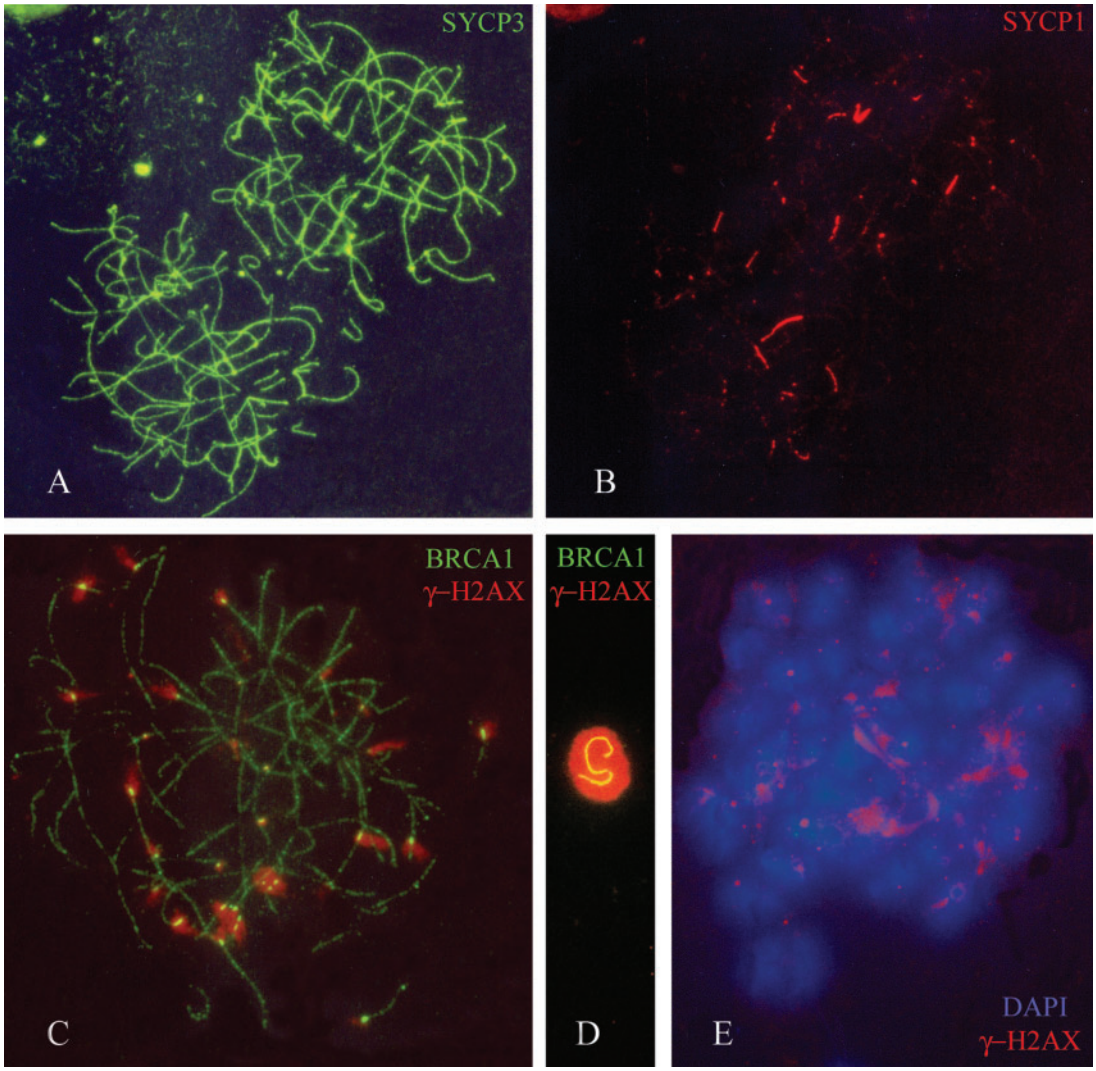

Figure 6. (**A**–**E**) Immunolocalization of meiotic proteins. (**A**) Immunolocalization of SYCP3 on two zygotene-like (centre) and one leptotene (upper left) spermatocytes. (**B**) Localization of SYCP1 (transverse filament protein) on the same cells. Only terminal patches of SYCP1 are seen. Magnification: ×1100. (**C**) Double immunolocalization of BRCA1 (on the single axes) and γ-H2AX (red patches on chromatin) on the zygotene-like spermatocyte nuclei. Magnification: ×1800. (**D**) Double immunolocalization (BRCA1 and γ-H2AX) on a control human spermatocyte. Only the XY body shows γ-H2AX labelling (red chromatin) and BRCA1 (differential X and Y axes). Magnification: ×1400. (**E**) Immunolocalization of γ-H2AX (red patches) on many of the chromosomes of one abnormal spermatocyte division. Magnification: ×1100.

(Figure 7A), in this patient RAD51 gave no signal at all in the zygotene-like spermatocytes (Figure 7B). Rad51 was absent in other types of germ cells as well.

Immunolocalization of MLH1

While in control human spermatocytes, MLH1 foci were present in all the pachytene bivalents, at the expected sites and numbers of crossovers (Figure 7C), in this patient MLH1 gave no signal at all in all the germ cells (Figure 7D).

Discussion

Synaptic failure in human spermatocytes

This case differs from the 'megalospermatocytes' described by Johannisson *et al*. (2003) in three azoospermic men. First, while megalospermatocytes show a predominance of asynaptic chromosomes, some of them also show the full synapsed complement. Second, the megalospermatocytes fail to progress but disintegrate, while in this case the abnormal zygotene spermatocytes revert in a sizable number to the abnormal cell divisions. Furthermore, the large diameter of megalospermatocyte nuclei (up to 17 μm; Johannisson *et al*., 2003) is larger than that of the abnormal zygotenes, and the nuclear contents are not so washed out. Although it is possible that megalospermatocytes may share some of the processes described in this case, the latter seems more homogeneous and more suggestive of a genetic disturbance. This case seems also to differ from the two patients found with a putative bp deletion in the gene *SYCP3* (Miyamoto *et al*., 2003), as these patients do not show abnormal spermatocyte divisions. The spermatogenic arrest in a patient attributed to the failure of formation of mature synaptonemal complexes (Judis *et al*., 2004) is also different, as no evidence was found of SYCP1 transverse filaments.

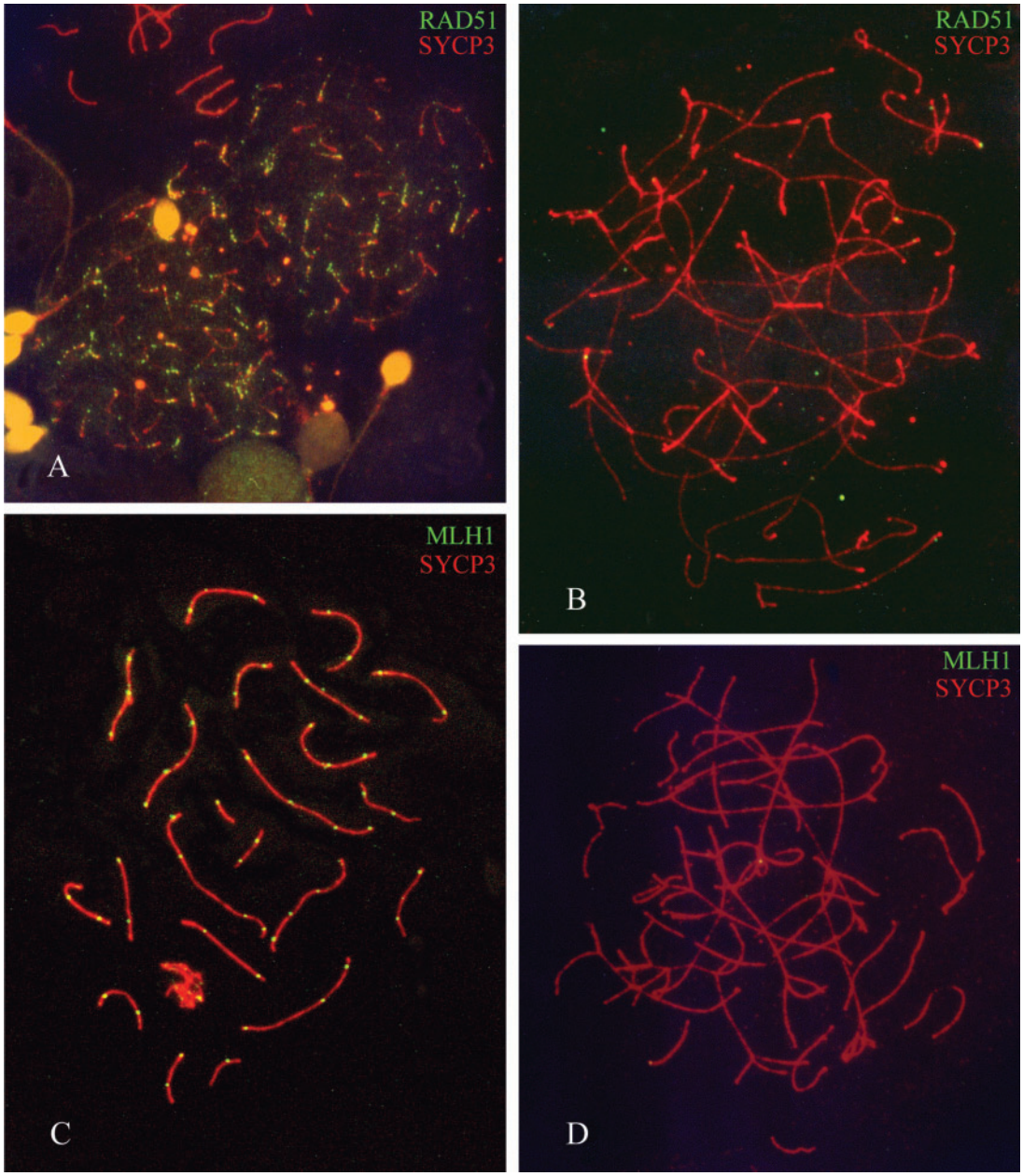

Figure 7. (**A**–**D**) Immunolocalization of RAD51 and MLH1 in the patient and in human control spermatocytes. (**A**) RAD51 in a normal control, showing the RAD51 foci on two leptotene cells (centre). One pachytene (upper left) spermatocyte has no RAD51 foci. Magnification: ×1100. (**B**) Double immunolocalization of SYCP3 and RAD51 on the zygotene-like cells of the patient. There is no labelling of RAD51. Magnification: ×1800. (**C**) Double immunolocalization (SYCP3 and MLH1) in a normal human spermatocyte. The MLH1 foci appear at the expected locations. Magnification: ×1400. (**D**) Double immunolocalization (SYCP3 and MLH1) in the zygotene-like cells of the patient. There are no foci of MLH1. Magnification: ×1400.

In this case, synaptic failure is not because of the absence of SYCP3, as all axes show a perfect immunolocalization of this protein. Neither the failure is because of a total absence of SYCP1, as this protein of the intermediate filaments is visible in many spermatocytes, mainly as short stretches near the chromosome termini (see *Results*).

While the single axes are fully formed and short stretches of synapsis appear, non-homologous synapsis has been documented (see *Results*). Thus, homologous, proper synapsis may not occur except at some chromosome termini. Furthermore, there is a full absence of the normal XY body, which suggests that the pseudoautosomal region in the XY pair fails to synapse.

This generalized failure of homologous synapsis suggests that a basic molecular mechanism of meiosis is impaired. The presence of the pericentric inversion in chromosome 2, inherited from the patient's mother, seems irrelevant for its spermatogenesis arrest. A search in the human genome database (NCBI, NIH) did not reveal any gene located in the fracture points that could be involved in meiosis arrest.

DSBs and their processing in mammalian spermatocytes

Meiotic recombination begins in many eukaryotes, including mammals (Mahadevaiah *et al*., 2001), through the induction of regulated, DSBs of the meiocyte DNA at leptotene (reviewed by Keeney, 2001). These DSBs occur by the action of a protein complex in which the leading factor is SPO11, a widely conserved protein (Keeney, 2001). The leading role of the protein SPO11 has been supported by several observations, especially the homozygous null mutation Spo11–/–, which leads to meiotic arrest and spermatocyte apoptosis (Baudat *et al*., 2000; Romanienko and Camerini Otero, 2000). In Spo11–/–, most subsequent steps of meiosis are deficient, especially the recruitment of RAD51 and DMC1 over the DNA ends, which define the beginning of DSBs processing (Baudat *et al*., 2000). A suitable marker of DSBs, both from meiocytes and from somatic cells subjected to radiation (inducing DSBs), is the appearance of a variant histone phosphorylated at serine 139, γ-H2AX (Mahadevaiah *et al*., 2001; reviewed in Redon *et al*., 2002). The fact that γ-H2AX begins to be located in patches over chromatin very shortly after irradiation (reviewed in Redon *et al*., 2002) means that it gives a good record of DSBs location. Furthermore, null mutations for γ-H2AX lead to radiation sensitivity and male sterility (Celeste *et al*., 2002).

On this basis, this patient shows a protein phenotype compatible with a deficiency of DSBs processing, and this deficiency occurs at the early steps of this processing. The DSBs marker, γ-H2AX, is present from leptotene and goes on localized on the single axes at the abnormal zygotenes (see *Results*). The lack of RAD51 labelling should mean that the RAD51–DMC1 protein complex is not recruited for DSB processing. As Rad51 null mutations are embryonic lethals (Tsuzuki *et al*., 1996), a complete deficiency of RAD51 is not likely to be present in this patient. Furthermore, Dmc1–/– null mutants show a different protein phenotype (Pittman *et al*., 1998). While Dmc1–/– show asynapsis and lack of XY body formation (Yoshida *et al*., 1998; Barchi *et al*., 2005), RAD51 labelling is present at leptotene–zygotene (Pittman *et al*., 1998), and they do not revert to abnormal cell divisions as described in this study.

Another null mutant which shares some of the features with the present case is Msh5–/–. However, null mutants for MSH5 do show RAD51 labelling (Edelmann *et al*., 1999) and do not advance to abnormal cell divisions.

Thus, it is suggested that the SPO11 protein complex, although allowing the production of DSBs, lacks some of the recruiting ability needed for the RAD51–DMC1 processing of broken ends.

This deficiency is maintained throughout prophase, including the chromosomes of the abnormal spermatocyte divisions. This deficiency may be the basis for inability of synaptic completion, the lack of MLH1 foci and, consequently, the lack of crossing over and chiasmata at the abnormal cell divisions.

XY body formation and its relationship with spermatogenesis arrest

Recently, the formation of the XY body (Solari, 1974, 1993) has been singled out from other meiotic processes (Barchi *et al*., 2005; Turner *et al*., 2005).

For three decades, it has been known that abnormalities of the XY body are associated with spermatogenesis impairment (Solari, 1993, 1999). Recently, the presence of BRCA1 in the differential regions of the X and Y axes has been associated with the special asynaptic state of these chromosomal regions (Turner *et al*., 2004, 2005). BRCA1 is present as a regulatory protein in the processing of DSBs in somatic (reviewed in Venkitaraman, 2002) and meiotic cells (Xu *et al*., 2003). The presence of BRCA1 along the unpaired axes in the present case suggests that BRCA1 is secondary to the lack of RAD51–DMC1 processing, which is lacking in this patient. On the other hand, while BRCA1 is present throughout the asynaptic axes, there is no formation of an XY body (see *Results*). However, several patches of evenly packed chromatin, resembling the chromatin of the XY body, are dispersed on the spermatocyte nucleus, in coincidence with γ-H2AX patches (see *Results*). This result resembles that of Spo11–/–, Dmc1–/– and Msh5–/– null mutants (Barchi *et al*., 2005), in which a 'pseudoXY body' or several similar chromatin bodies have been observed (Barchi *et al*., 2005). The XY body is labelled at pachytene with γ-H2AX in normal spermatocytes (Mahadevaiah *et al*., 2001). Many other proteins are located at the normal XY body (reviewed in Handel, 2004), but the real importance of γ-H2AX in the formation of this body is suggested by the failure of XY body formation in H2AX null mice (Fernandez-Capetillo *et al*., 2003). Recent work has suggested the presence of three separate pathways for γ-H2AX formation (phosphorylation of H2AX at serine 139). H2AX phosphorylation in the XY body is attributed to the ataxia-telangiectasia Rad3 (ATR)-related protein kinase (Turner *et al*., 2004, 2005), whereas the formation of γ-H2AX patches over the chromatin with DSBs of leptotene–zygotene cells is attributed to the AT-mutated (ATM) protein kinase (Barchi *et al*., 2005). A third pathway for H2AX phosphorylation occurs in pre-meiotic cells, during DNA replication, and is not related to meiotic processes (Turner *et al*., 2004).

The prior presence of BRCA1 in the axes of the XY would be needed for the recruitment of the kinase ATR and the formation of the γ-H2AX dominion on the XY body (Turner *et al*., 2004, 2005). In the absence of DSBs in Spo11 null mutants, these pathways are inhibited and there are no γ-H2AX patches and no formation of the XY body (Bellani *et al*., 2005). Furthermore, Dmc1 and Msh5 null mutants also inhibit XY body formation, but they do not preclude the formation of patches of γ-H2AX over chromatin having non-processed DSBs (Barchi *et al*., 2005).

In this case, the XY body formation is inhibited but γ-H2AX patches are present from leptotene up to the abnormal cell divisions, and RAD51 foci are absent. This protein phenotype neither overlaps completely with Dmc1 and Msh5 mutants (Barchi *et al*., 2005) nor is compatible with the full effects of a null Spo11 mutation (lack of DSBs). Thus, it is suggested that while DSBs do occur in this patient, the recruitment of the needed proteins for the next steps in DSBs processing (recruitment of proteins that modifies the broken ends of DNA and/or makes the RAD51-DMC1 complex accessible) is deficient in this patient.

Mitotic-like reversion of abnormal meiocytes

To the best of our knowledge, there are no reports of human meiotic cells reverting to a mitosis-like division, as described in this study. The complete lack of crossing overs in these cells as shown by the lack of MLH1 foci agrees with the appearance of cells having a diploid number of separate chromosomes. These cells degenerate and die: as shown in *Results*, they do not have a microtubular apparatus for moving chromosomes, the cytoplasm is full of vacuoles and no chromosome orientation is observed. This ill-fate is not surprising in cells that have non-processed DSBs, as shown by the γ-H2AX marker (see *Results*). In this respect, the spermatocytes of this patient, which reach a last stage in the abnormal divisions, are different from the yeast cells that can reverse meiosis and enter a mitotic growth phase (Honigberg and Esposito, 1994). Thus, the abnormal spermatocyte divisions should not be equalled to mitoses, as they are unequivocally dying cells, although they resemble mitotic divisions when observed with light microscopy.

Impact of genetic failures in human spermatogenesis

This case as well as two other recent papers (see *Introduction*) strengthens the view that human spermatogenesis is subjected to several types of meiotic failures, whose molecular detail and mechanism is only beginning to be understood. The important advances recently made on the mechanisms of meiotic prophase in the mouse (see *Introduction*) are guides for the next advances in the understanding of human spermatogenic arrest.

Acknowledgements

We thank Dr Peter B. Moens and Barbara Spyropoulos (York University, Ontario, Canada) for the generous gift of antibodies, SYCP1 and SYCP3. We thank the able technical help of Cristina Deparci (CIR) and the staff of CEGYR. R.B.S. is a fellow from Conicet, and M.I.P. and A.J.S. are members of the Carrera del Investigador. M.I.R. is Profesional de Apoyo (Conicet). We thank the grants from UBACYT (M 008) and Conicet (2137).

References

Barchi M, Mahadevaiah S, Di Giacomo M, Baudat F, de Rooij DG, Burgoyne PS, Jasin M and Keeney S (2005) Surveillance of different recombination defects in mouse spermatocytes yields distinct responses despite elimination at an identical developmental stage. Mol Cell Biol 25,7203–7215.

Baudat F, Manova K, Yuen JP, Jasin M and Keeney S (2000) Chromosome synapsis defects and sexually dimorphic meiotic progression in mice lacking Spo11. Mol Cell 6,989–998.

Bellani MA, Romanienko PJ, Cairatti DA and Camerini-Otero D (2005) SPO11 is a required for sex-body formation, and Spo11 heterozygosity rescues the prophase arrest of $Atm^{-/-}$ spermatocytes. J Cell Sci 118,3233–3245.

Celeste A, Petersen S, Romanienko PJ, Fernandez-Capetillo O, Chen HT, Sedelnikova OA, Reina-San-Martin B, Coppola B, Meffre E, Difilippantonio MJ *et al*. (2002) Genomic instability in mice lacking histone H2AX. Science 296,922–927.

de Vries S, Baart EB, Dekker M, Siezen A, de Rooij DG, de Boer P and te Riele H (1999) Mouse MutS-like protein Msh5 is required for proper chromosome synaposis in male and female meiosis. Genes Dev 13,523–531.

Edelmann W, Cohen PE, Kane M, Lau K, Morrow B, Bennett S, Umar A, Kunkel T, Cattoretti G, Chaganti R *et al*. (1996) Meiotic pachytene arrest in MLH1-deficient mice. Cell 85,1125–1134.

Edelmann W, Cohen PE, Kneitz B, Winand N, Lia M, Heyer J, Kolodner R, Pollard JW and Kucherlapati R (1999) Mammalian MutS homologue 5 is required for chromosome pairing in meiosis. Nat Genet 21,123–127.

Escalier D (2001) Impact of genetic engineering on the understanding of spermatogenesis. Hum Reprod Update 7,191–210.

Fernandez-Capetillo O, Mahadevaiah SK, Celeste A, Romanienko PJ, Camerini-Otero RD, Bonner WM, Manova K, Burgoyne P and Nussenzweig A (2003) H2AX is required for chromatin remodeling and inactivation of sex chromosomes in male mouse meiosis. Dev Cell 4,497–508.

Handel MS (2004) The XY body: a specialized meiotic chromatin domain. Exp Cell Res 296,57–63.

Honigberg SM and Esposito RE (1994) Reversal of cell determination in yeast meiosis: postcommitment arrest allows return to mitotic growth. Proc Natl Acad Sci USA 91,6559–6563.

Howell WM and Black DA (1980) Controlled silver staining of nucleolus organizer regions with a protective colloidal developer: a 1 step method. Experientia 36,1014–1015.

Johannisson R, Schluze W and Holstein AF (2003) Megalospermatocytes in the human testis exhibit asynapsis of chromosomes. Andrologia 35,146–151.

Judis L-A, Chan ER, Schwartz S, Seftel A and Hassold T (2004) Meiosis I arrest and azoospermia in an infertile male explained by failure of formation of a component of the synaptonemal complex. Fertil Steril 81,205–209.

Keeney S (2001) Mechanism and control of meiotic recombination initiation. Curr Top Dev Biol 52,1–53.

Kolas NK, Marcon E, Crackower MA, Hoog C, Penninger JM, Spyropoulos B and Moens PB (2005) Mutant meiotic chromosome core components in mice can cause apparent sexual dimorphic endpoints at prophase or X-Y defective male-specific sterility. Chromosoma 114,92–102.

Mahadevaiah SK, Turner JMA, Baudat F, Rogakou EP, de Boer P, Blanco-Rodriguez J, Jasin M, Keeney S, Bonner WM and Burgoyne PS (2001) Recombinational DNA double-strand breaks in mice precede synapsis. Nat Genet 27,271–276.

Masson J-Y and West SC (2001) The Rad51 and Dmc1 recombinases: a non-identical twin relationship. Trends Biochem Sci 26,131–136.

Miyamoto T, Hasulke S, Yogev L, Maduro MR, Ishikawa M, Westphal H and Lamb DJ (2003) Azoospermia in patients heterozygous for a mutation in SYCP3. Lancet 362,1714–1719.

Pittman DL, Cobb J, Schimenti KJ, Wilson LA, Cooper DM, Brignull E, Handel MA and Schimenti JC (1998) Meiotic prophase arrest with failure of chromosome synapsis in mice deficient for Dmc1, a germline-specific RecA homolog. Mol Cell 1,697–305.

Redon C, Pilch D, Rogakou E, Sedelnikova O, Newrock K and Bonner W (2002) Histone H2A variants H2AX and H2AZ. Curr Opin Genet Dev 12,162–169.

Romanienko PJ and Camerini-Otero RD (2000) The mouse Spo11 gene is required for meiotic chromosome synapsis. Mol Cell 6,975–987.

Schulze W, Thoms F and Knuth UA (1999) Testicular sperm extraction: comprehensive analysis with simultaneously performed histology in 1418 biopsies from 766 subfertile men. Hum Reprod 14 (Suppl. 1),82–96.

Solari AJ (1974) The behaviour of the XY pair in mammals. Int Rev Cytol 38,273–317.

Solari AJ (1980) Synaptonemal complexes and associated structures in microspread human spermatocytes. Chromosoma 81,315–337.

Solari AJ (1993) *Sex Chromosomes and Sex Determination in Vertebrates*. CRC Press, Boca Raton, FL.

Solari AJ (1998) Structural analysis of meiotic chromosomes and synaptonemal complexes in higher vertebrates. In Berrios M (ed.) *Nuclear Structure and Function, Methods in Cell Biology*, Vol. 53. Academic Press, San Diego, CA, pp. 235–256.

Solari AJ (1999) Synaptonemal complex analysis in human male infertility. Eur J Histochem 43,265–276.

Solari AJ, Rahn MI, Saura A and Lujan HD (2003) A unique mechanism of nuclear division in Giardia lamblia involves components of the ventral disk and the nuclear envelope. Biocell 27,329–346.

Speed RM (1989) Heterologous pairing and fertility in humans. In Gillies CB (ed.), *Fertility and Chromosome Pairing: Recent Studies in Plants and Animals*. CRC Press, Boca Raton, FL, pp. 1–35.

Sun F, Kozak G, Scott S, Trpkov K, Ko E, Mikhaail-Philips M, Bestor TH, Moens P and Martin RH (2004) Meiotic defects in a man with non-obstructive azoospermia: case report. Hum Reprod 19,1770–1773.

Tsuzuki T, Fujii Y, Sakumi K, Tominaga Y, Nakao K, Sekiguchi M, Matsushiro A, Yoshimura Y and Morita T (1996) Targeted disruption of the Rad51 gene leads to lethality in embryonic mice. Proc Natl Acad Sci USA 93,6236–6240.

Turner JMA, Aprelikova O, Xu X, Wang R, Kim S, Chandramouli GVR, Barrett JC, Burgoyne PS and Deng C-X (2004) BRCA1, histone H2AX phosphorylation, and male meiotic sex chromosome inactivation. Curr Biol 14,2135–2142.

Turner JMA, Mahadevaiah SK, Fernandez-Capetillo O, Nussenzweig A, Xu X, Deng C-X and Burgoyne PS (2005) Silencing of unsynapsed meiotic chromosomes in the mouse. Nat Genet 37,41–47.

Van Assche E, Bonduelle M, Tournaye H, Joris H, Verheyen G, Devroey P, Van Steirteghem A and Liebaers I (1996) Cytogenetics of infertile men. Hum Reprod 11 (Suppl. 4),1–26.

Venkitaraman AR (2002) Cancer susceptibility and the functions of BRCA1 and BRCA2. Cell 108,171–182.

Xu Y, Ashley T, Brainerd EE, Bronson RT, Meyn MS and Baltimore D (1996) Targeted disruption of ATM leads to growth retardation, chromosomal fragmentation during meiosis, immune defects, and thymic lymphoma. Genes Dev 10,2411–2422.

Xu X, Aprelikova O, Moens PB, Deng C-X and Furth PA (2003) Impaired meiotic DNA-damage repair and lack of crossing-over during spermatogenesis in BRCA1 full-length isoform deficient mice. Development 130,2001–2012.

Yoshida K, Kondoh G, Matsuda Y, Habu T, Nishimune Y and Morita T (1998) The mouse RecA-like gene Dmc1 is required for homologous chromosome synapsis during meiosis. Mol Cell 1,707–718.

Yuan L, Liu JG, Zhao J, Brundell E, Daneholt B and Hoog C (2000) The murine SCP3 gene is required for synaptonemal complex assembly, chromosome synapsis, and male fertility. Mol Cell 5,73–83.

Submitted on October 6, 2005; resubmitted on November 25, 2005; accepted on December 6, 2005